View metadata, citation and similar papers at core.ac.uk

brought to you by CORE

provided by IntechOpen

We are IntechOpen, the world's leading publisher of Open Access books Built by scientists, for scientists

4,800
Open access books available

122,000
International authors and editors

135M
Downloads

Our authors are among the

154
Countries delivered to

TOP 1%
most cited scientists

12.2%
Contributors from top 500 universities

CLARIVATE ANALYTICS BOOK CITATION INDEX INDEXED

WEB OF SCIENCE™

Selection of our books indexed in the Book Citation Index in Web of Science™ Core Collection (BKCI)

Interested in publishing with us?
Contact book.department@intechopen.com

Numbers displayed above are based on latest data collected.
For more information visit www.intechopen.com

Chapter 8

Optical Properties of Ferroelectrics and Measurement Procedures

A.K. Bain and Prem Chand

Additional information is available at the end of the chapter

http://dx.doi.org/10.5772/52098

1. Introduction

It is well known that the optical properties of ferroelectric materials find wide ranging applications in laser devices. Particularly in the recent years, there has been tremendous interest in the investigation of the nonlinear optical properties of ferroelectric thin films [1-5] for planar waveguide and integrated –optic devices. A new class of thin film waveguides has been developed using $BaTiO_3$ thin films deposited on MgO substrates [6]. Barium strontium titanate $Ba_{1-x}Sr_xTiO_3$ (BST) is one of the most interesting thin film ferroelectric materials due to its high dielectric constant, composition dependent Curie temperature and high optical nonlinearity. The composition dependent T_c enables a maximum infrared response to be obtained at room temperature. The BST thin films in the paraelectric phase, have characteristics such as good chemical and thermal stability and good insulating properties, due to this nature they are often considered the most suitable capacitor dielectrics for successful fabrication of high density Giga bit (Gbit) scale dynamic random access memories (DRAMs). Compositionally graded ferroelectric films have exhibited properties not previously observed in conventional ferroelectric materials. The most notable property of the graded ferroelectric devices or graded Functionally Devices (GFDs) is the large DC polarization offset they develop when driven by an alternating electric field. Such GFDs can find applications as tunable multilayer capacitors, waveguide phase shifters and filters [7]. Recently, BST thin films were used in the formation of graded ferroelectric devices by depositing successive layers of BST with different Ba/Sr ratios [8].

In our work, the Barium strontium titanate ($Ba_{0.05}Sr_{0.95}TiO_3$) ferroelectric thin films were prepared on single crystal [001] MgO substrates using the pulsed laser deposition method. The refractive index of BST ($Ba_{0.05}Sr_{0.95}TiO_3$) thin films is determined in the wavelength range between 1450-1580 nm at the room temperature. The dispersion curve is found to decrease

INTECH
open science | open minds

© 2013 Bain and Chand; licensee InTech. This is an open access article distributed under the terms of the Creative Commons Attribution License (http://creativecommons.org/licenses/by/3.0), which permits unrestricted use, distribution, and reproduction in any medium, provided the original work is properly cited.

gradually with increasing wavelength. The average value of the refractive index is found to be 1.985 in the wavelength range between 1450-1580 nm which is important for optoelectronic device applications [9].

1: Present address: Director, PM College of Engineering, Kami Road, Sonepat-131001.

2: Present Address: 99 Cyril Road, Small Heath, Birmingham B10 0ST.

Lithium heptagermanate $Li_2Ge_7O_{15}$ (LGO) is regarded as a weak ferroelectric and its curie point T_c is 283.5K [10,11]. Due to its intermediate behaviour between order-disorder and displacive types in a conventional grouping of ferroelectric materials LGO remains a subject of interest from both the theoretical and the application point of view. The paraelectric phase above T_c is orthorhombic D^{14}_{2h} ~ pbcn and below T_c the ferroelectric phase is C^5_{2v} ~ $pbc2_1$ with four formula units in a unit cell in both the phases. Below T_c LGO shows dielectric hysteresis loop and the permittivity shows a sharp peak at T_c [10-12]. Below T_c the spontaneous polarization appears along the c-axis. Many interesting physical properties of LGO such as birefringence [13], elastic behaviour [14], thermal expansion [11], dielectric susceptibility [12,15, 16] and photoluminescence [17] exhibit strong anomalies around T_c. The optical properties, however vary only to such a small degree that the transition could not be detected with the aid of a standard polarization microscope [13]. Employing a high resolution polarization device, Kaminsky and HaussÜhl [13] studied the birefringence in LGO near T_c and observed anomalies at the phase transition.

The study of piezo-optic dispersion of LGO (un-irradiated and x-irradiated) in the visible region of the spectrum of light at room temperature (RT=298 K) shows an optical zone/ window in between 5400Å and 6200Å with an enhanced piezo-optical behavior [18]. The temperature dependence of the photoelastic coefficients of the ferroelectric crystals $Li_2Ge_7O_{15}$ (both un-irradiated and x-irradiated) in a cooling and a heating cycle between room temperature and 273K shows an interesting observation including the lowering of the T_c under uniaxial stress contrary to the increase of T_c under hydrostatic pressure and observation of thermal photoelastic hysteresis similar to dielectric behavior [19]. The study of fluorescence spectra of the crystals $Li_2Ge_7O_{15}:Cr^{3+}$ in the temperature interval 77-320 K shows the sharply decrease of intensities of the R_1 and R_2 lines (corresponding to the Cr^{3+} ions of types I and II) during cooling process near the temperature T_c = 283.5 K[16].

The present chapter includes optical properties of the ferroelectric BST thin films and the Lithium heptagermanate ($Li_2Ge_7O_{15}$) single crystals, fabrication methods, measurement procedures of the refractive index of BST thin films on MgO substrates, the fluorescence spectra and the photoelastic coefficients of LGO single crystals (un-irradiated and x-irradiated) at different wave lengths and temperatures around the phase transition temperature T_c. The potential of these materials for practical applications in the opto-electronic devices will also be discussed.

1.1. Optical property of Barium strontium titanate thin films

The Barium strontium titanate ($Ba_{0.05}Sr_{0.95}TiO_3$) ferroelectric thin films were prepared on single crystal MgO substrates using the pulsed laser deposition (PLD) method at a substrate

http://dx.doi.org/10.5772/52098

temperature of 780 °C and then annealed at 650 °C for 55 min. The x-ray diffraction (XRD) analysis revealed that the films are oriented with [001] parallel to the substrate [001] axis and thus normal to the plane of the films [9]. The films were grown to a thickness of 430 nm.

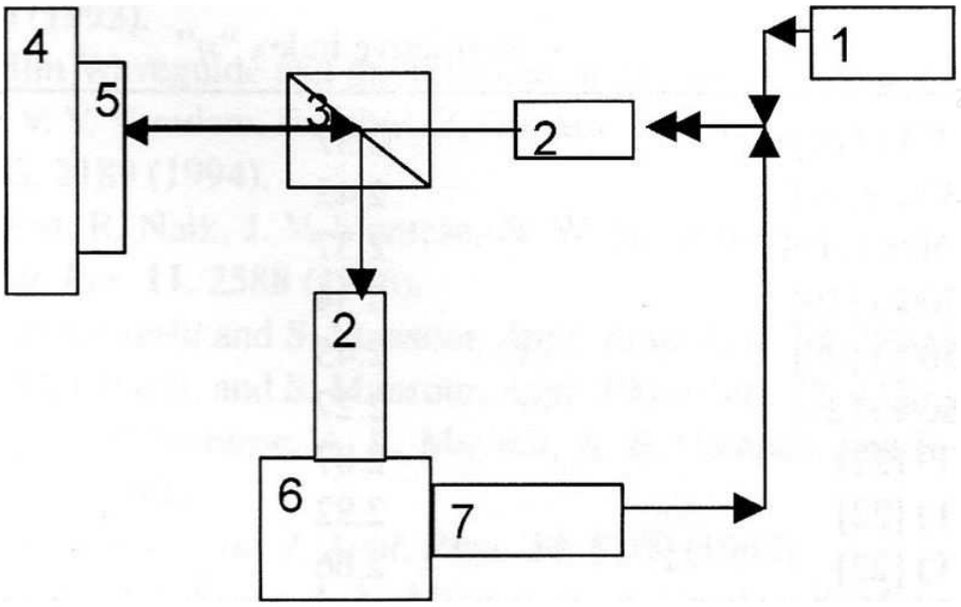

Figure 1. Schematic diagram of the experimental setup for the measurement of refractive index of the $Ba_{0.05}Sr_{0.95}TiO_3$ thin films at room temperature. He-Ne Laser for alignment (1), Lenses (2), Polarizer (3), sample holder (4), BST sample (5), Agilent light wave measurement system (6) and Tunable Laser (7).

Figure 1 shows the schematic diagram of the experimental setup for the measurement of the refractive index of $Ba_{0.05}Sr_{0.95}TiO_3$ thin films on MgO substrates through a reflection method. The He-Ne laser beam is used as a source of light to setup the alignment of the reflected beam of light from the samples to the detector. The incident beam is allowed to pass through a polarizer onto the sample. The reflected light is then passed through the same polarizing beam splitter oriented at 45° relative to the incident light and finally allowed to fall on the detector that is at 90° to the reflected/incident beam of light. The reflectivity measurement of the black metal, mirror, MgO substrate and $Ba_{0.05}Sr_{0.95}TiO_3$ thin films were carried using the Agilent 8164A Light Wave Measurement system in the wavelength region of 1450-1580 nm at room temperature.

The refractive index of substrate MgO is taken to be 1.7 [9]. The reflectivity of $Ba_{0.05}Sr_{0.95}TiO_3$ film is then normalized with respect to the mirror. The value of refractive index is derived from model described in ref. [20]. The fitting is done with the calculated data of the reflectivity of $Ba_{0.05}Sr_{0.95}TiO_3$ in the wavelength range between 1450-1580 nm. Figure 2 shows the refractive index of $Ba_{0.05}Sr_{0.95}TiO_3$ thin films as a function of wavelength at room temperature. The refractive index of $Ba_{0.05}Sr_{0.95}TiO_3$ with $Ba_xSr_{1-x}TiO^3$ (BST) and other materials of ferroelectric thin films at different wavelengths are presented in table 1.

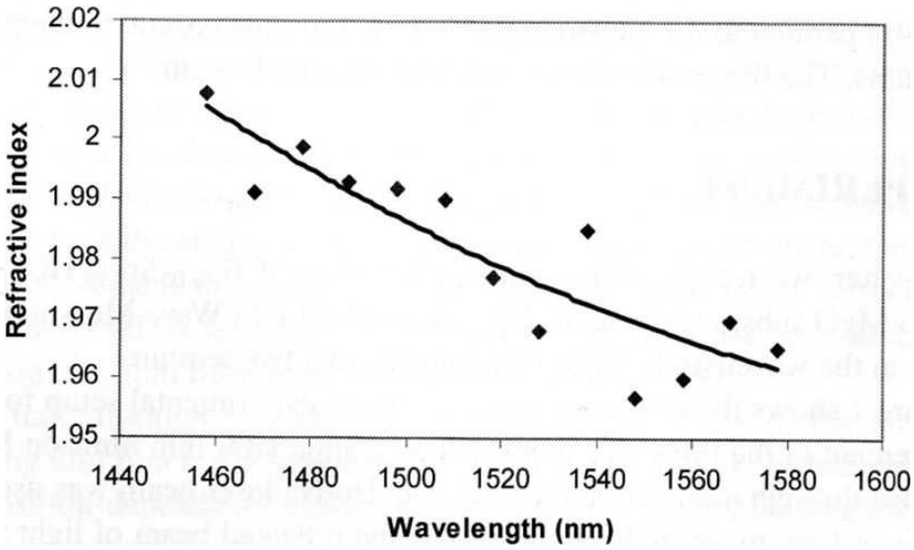

Figure 2. The variation of refractive index of $Ba_{0.05}Sr_{0.95}TiO_3$ thin films as a function of wavelength.

Sample Name	Refractive index	Wavelength	Remarks
$Ba_xSr_{1-x}TiO3(x=0\%)$	2.37	600 nm (RT)	Ref. [21]
$Ba_xSr_{1-x}TiO3(x=30\%)$	2.42	600 nm (RT)	Ref. [21]
$Ba_xSr_{1-x}TiO3(x=50\%)$	2.37	600 nm (RT)	Ref. [21]
$Ba_xSr_{1-x}TiO3(x=70\%)$	2.34	600 nm (RT)	Ref. [21]
$Ba_xSr_{1-x}TiO3(x=50\%)$	2.45	470 nm (RT)	Ref. [22]
$Ba_xSr_{1-x}TiO3(x=80\%)$	2.27	430 nm (RT)	Ref. [23]
$PbZr_{1-x}Ti_xO3$ (PZT)	2.87	400 nm (300 ^{0}C)	Ref. [24]
$PbZr_{1-x}Ti_xO3$ (PZT)	2.82	400 nm (50 ^{0}C)	Ref. [24]
$PbZr_{1-x}Ti_xO3$ (PZT)	2.66	500 nm (300 ^{0}C)	Ref. [24]
$PbZr_{1-x}Ti_xO3$ (PZT)	2.67	500 nm (50 ^{0}C)	Ref. [24]
$PbTiO_3$	3.10	470 nm (RT)	Ref. [25]
$PbTiO_3$	2.80	490 nm (RT)	Ref. [25]
$PbTiO_3$	2.75	550 nm (RT)	Ref. [25]
$Sr_xBa_{1-x}Nb_2O_6$ (x=61%)	2.35	400 nm (RT)	Ref. [26]

Table 1. The refractive index of BST and other ferroelectric thin films.

As shown in Figure 2, the dispersion curve decreases gradually with increasing wavelength. The average value of the refractive index is found to be ~ 1.985 in the wavelength range of 1450-1580 nm which is important for optoelectronic device (optical waveguide) applications. The variation of refractive index is attributed predominantly to the changes of electronic

http://dx.doi.org/10.5772/52098

structure associated with the larger lattice parameter and variations in atomic co-ordination [27] that is local relaxations.

1.2. Growth and structure of $Li_2Ge_7O_{15}$ Crystals

Single crystals of $Li_2Ge_7O_{15}$ are grown in an ambient atmosphere by Czochralski method from stoichiometric melt, employing a resistance heated furnace. Stoichiometric mixture of powdered Li_2CO_3 and GeO_2 in the ratio of 1.03 and 7.0 respectively was heated at 1100 K for 24 hours to complete the solid state reaction for the raw material for the crystal growth. The crystals were grown by rotating the seed at the rate of 50 rpm with a pulling rate of 1.2 mm/hour. The cooling rate of temperature in the process of growth was 0.8-1.2 K/hour. The crystals grown were colourless, fully transparent and of optical quality. The crystal axes were determined by x-ray and optical methods.

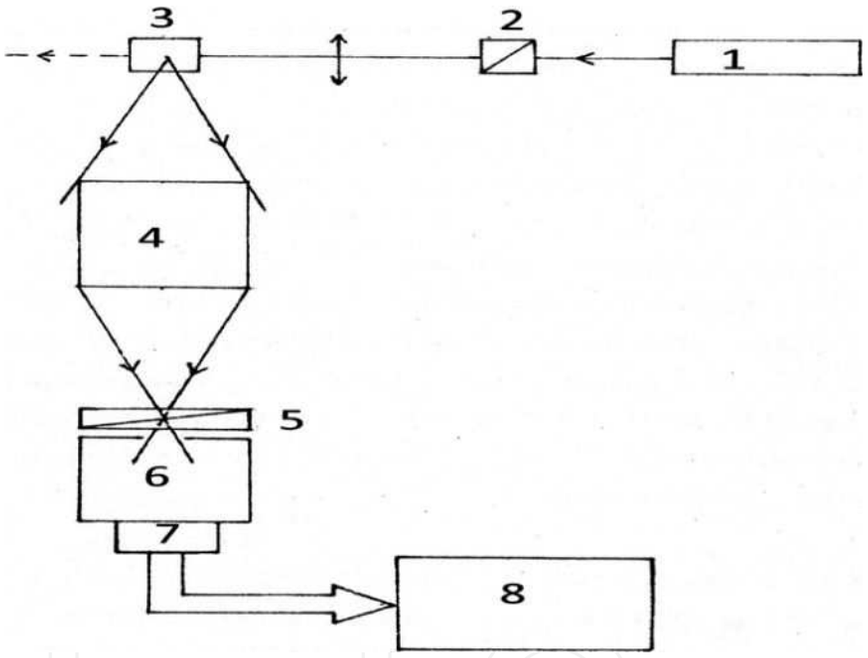

Figure 3. Schematic diagram of the experimental setup for the measurement of fluorescence spectra of the crystals $Li_2Ge_7O_{15}:Cr^{3+}$. He-Ne Laser for radiation (1), Glen prism (2), crystal sample (3), condenser (4), polarizer (5), spectrograph (6) Multichannel analyzer(7) and computer (8).

The desired impurities such as Cr^{+3}, Mn^{+2}, Bi^{+2}, Cu^{2+} and Eu^{+2} etc are also introduced in desired concentration by mixing the appropriate amount of the desired anion salt in the growth mixture. The crystal structure of LGO above T_c is orthorhombic (psedohexagonal) with the space group $D^{14}{}_{2h}$ (Pbcn). The cell parameters are a: 7.406 Å, b: 16.696 Å, c: 9.610 Å, Z = 4 and b~√3c. Below T_c a small value of spontaneous polarization occurs along c-axis and the ferroelectric phase belongs to $C^5{}_{2v}$ ($Pbc2_1$) space group. The crystal structure contains strongly packed layers of GeO_4 tetrahedra linked by GeO_6-octahedra to form a three dimensionally bridged frame work in which Li atoms occupy the positions in the vacant channels extending three dimensionally [14, 28, 29]. The size of the unit cell (Z = 4) does not change at

the phase transition and ferroelectric phase transition is associated with a relaxational mode as well as the soft phonon [30]. Activation of the pure crystals with impurity ions will demand charge compensating mechanism through additional defects in the pure lattice.

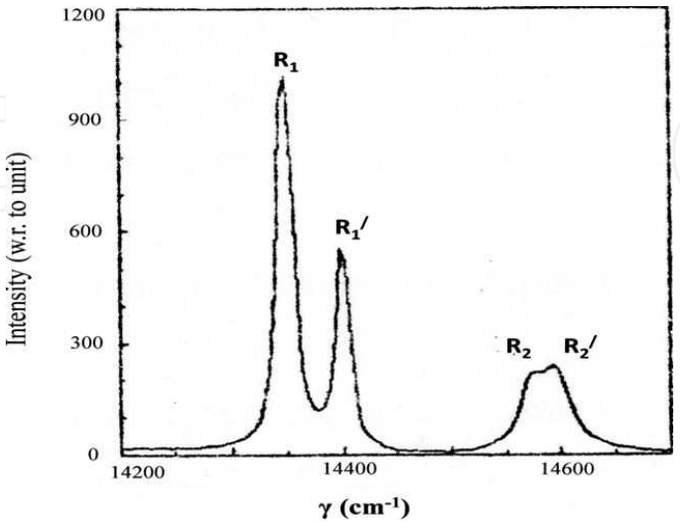

Figure 4. Fluorescence Spectra of the crystals $Li_2Ge_7O_{15}:Cr^{3+}$ at T=77 K.

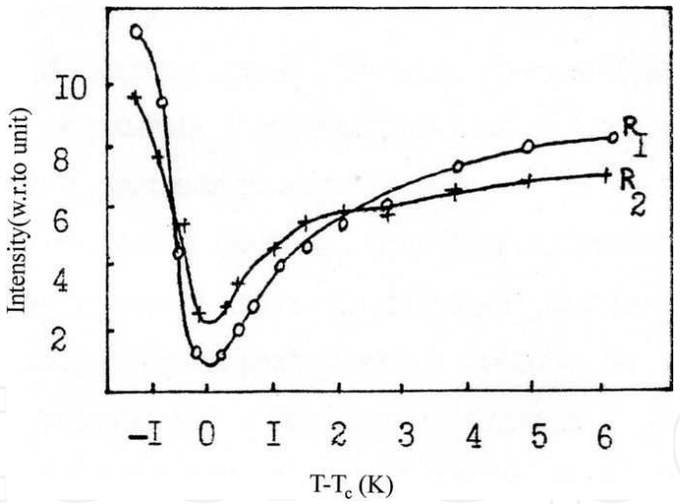

Figure 5. Temperature dependence of intensity of R_1 and R_2 Lines of fluorescence in $Li_2Ge_7O_{15}:Cr^{3+}$ crystals near the phase transition temperature T_c.

1.3. Study of fluorescence spectra of $Li_2Ge_7O_{15}:Cr^{3+}$ crystals

The fluorescence spectra of the crystals $Li_2Ge_7O_{15}:Cr^{3+}$ were studied in the temperature interval 77-320 K including the phase transition temperature T_c = 283.5 K. The experimental set to record the fluorescence spectra of the crystals $Li_2Ge_7O_{15}:Cr^{3+}$ is shown in fig.3. A laser with the pair of mode (λ_1=510.6 nm, λ_2=578.2 nm) was used as a source of excitation of the crystal

http://dx.doi.org/10.5772/52098

sample. The recording of fluorescence spectra were carried out by the optical multichannel analyzer in combination with the polychromator. The radiation beam was initially polarized with glen prism. The plane Polaroid was used as an analyzer that was placed before the input aperture of the polychromator.

The fluorescence spectra consist of narrow intensity lines referred to R_1 and R_2 with frequencies γ_1~14348 cm^{-1} and γ_2 ~14572 cm^{-1}. These lines split further into two components each R_1 / and R_2 / respectively at lowering the temperature towards 77 K. Besides this, a wide long wavelength region/zone is observed in the spectra. It may be related with the effect of electron-photon interaction. It is known that Cr^{3+} doping ions in the structure of $Li_2Ge_7O_{15}:Cr^{3+}$ crystals substitute the Ge^{4+} host ions within oxygen octahedral (GeO_6) complexes [31-36]. The optical spectra of Cr^{3+} ions shows the existence of two types of Cr^{3+} centre (type I and II with different values of effective g-factor) as observed in EPR (Electron Paramagnetic Resonance) spectra of Cr^{3+} ions in ferroelectric phase of the crystals $Li_2Ge_7O_{15}:Cr^{3+}$ [32, 33]. Two pair of R lines $4A_2$ - ^2E (at T=77 K, its positions are R_1=14348 cm^{-1}, R_1 /=14402 cm^{-1}, R_2=14572 cm^{-1} and R_2 /=14593 cm^{-1}) are observed at low temperature region (T<190 K) in the optical spectra of the crystals $Li_2Ge_7O_{15}:Cr^{3+}$ as shown in Fig. 4. Actually the two different types of Cr^{3+} centers (R and R/) with pretty different positions below $\bar{E}$ and above $2\bar{A}$ levels of the excited E^2 level are duplicate [37, 38] and conform to the EPR observations.

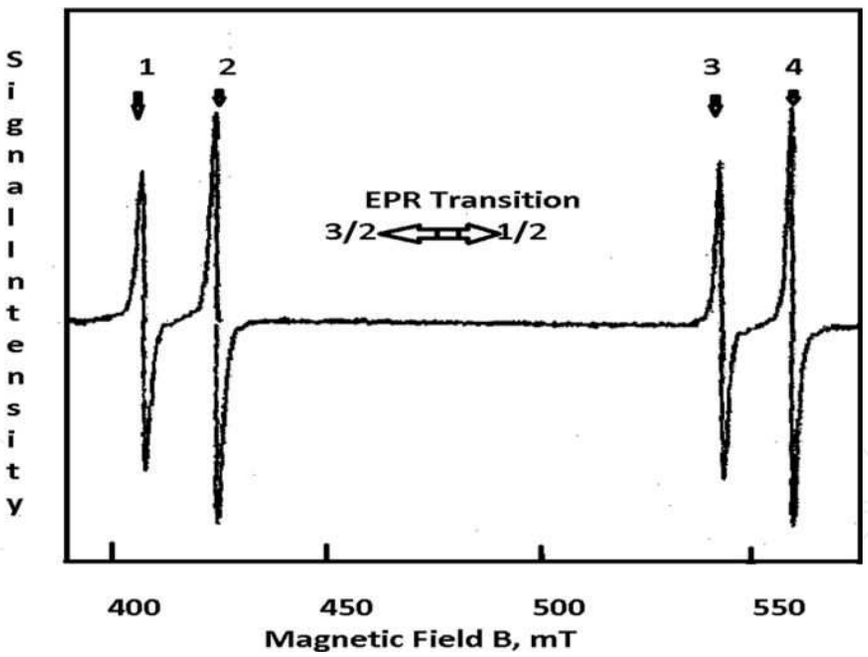

Figure 6. Part of EPR spectrum of Cr^{3+} doped LGO crystal in an arbitrary orientation at RT. The four EPR signals are attributed to four distinct Cr^{3+} sites per unit cell of LGO.

The intensity of fluorescence of the R_1 and R_2 lines of the crystals $Li_2Ge_7O_{15}:Cr^{3+}$ were studied near the phase transition temperature T_c at the direction E⊥[001]. It is observed that the intensity of R_1 and R_2 lines are decreased sharply near the phase transition temperature T_c but at high temperature region ($T>T_c$) the intensity again increases as shown in figure 5. Such

nature of suppression of R_1 and R_2 lines was not observed previously and it may be related with the mechanism of interaction of excitation spectra of light in the crystals $Li_2Ge_7O_{15}:Cr^{3+}$ near the phase transition temperature T_c[17].

The Crystals doped with chromium impurity give EPR (Electron Paramagnetic Resonance) signals characteristics of the trivalent chromium ions [Fig.6]. It is known that impurity Cr^{3+} ions substitute the Ge^{4+} host ions within oxygen octahedral in the basic structure of (LGO) crystal [31-36]. Incorporation of tri-positive chromium ions into GeO_6-octahedra changes the local symmetry of the lattice site from monoclinic C_2 group to triclinic C_1 group. The local symmetry lowering is attributed to the effect of the additional Li^+ defect required for compensating the charge misfit of Cr^{3+} ion at the Ge^{4+} site. Taking into account a weak coupling of lithium ions with the germanium – oxygen lattice framework, the interstitial Li^+ is considered to be the most probable charge compensating defect, located within the structural cavity near the octahedral CrO_6 complex (Fig.7). Subsequent measurements of optical spectra have confirmed the model of Cr^{3+}– Li^+ pair centers in the LGO crystal structure [32, 33].

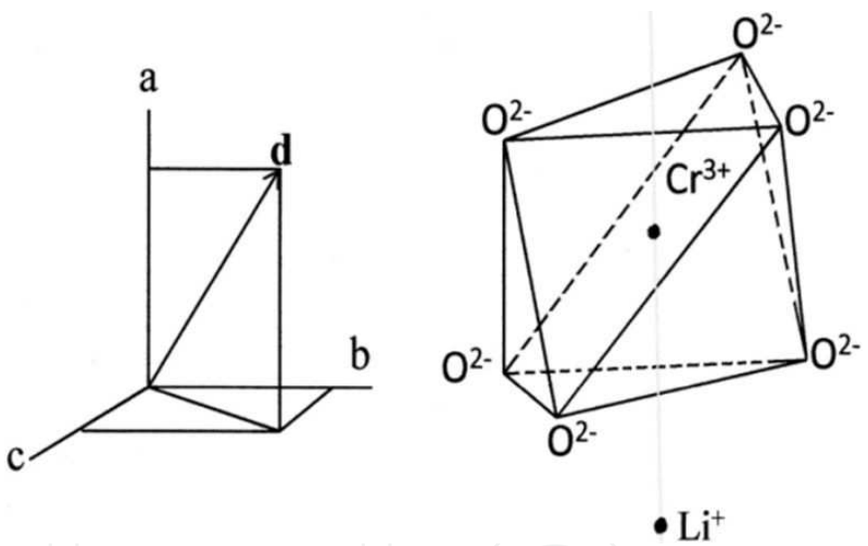

Figure 7. Physical model of Cr^{3+} centers in $Li_2Ge_7O_{15}:Cr^{3+}$ crystals and its dipole moment d.

The available data make it possible to assume that electric dipole moments of Cr^{3+}– Li^+ pairs are directed along the crystal axis "a" of the crystal. Interstitial Li^+ ions locally break the symmetry axis C_2 of the sites within the oxygen octahedral complexes [34]. As a result, there are two equivalent configurations of the pair centers which are conjugated by broken C_2 axis and have dipole moments with opposite orientations. It may be assumed that pair centers can reorient due to thermal activation. Reorientation of the pair centers should be accompanied by: i) shortening of the configuration life time and ii) switching of defect dipole moments [35]. This is reflected in the typical temperature dependence of the imaginary part of dielectric permittivity of chromium doped LGO single crystals [35] along the a-axis of the crystal shown in fig.8.

http://dx.doi.org/10.5772/52098

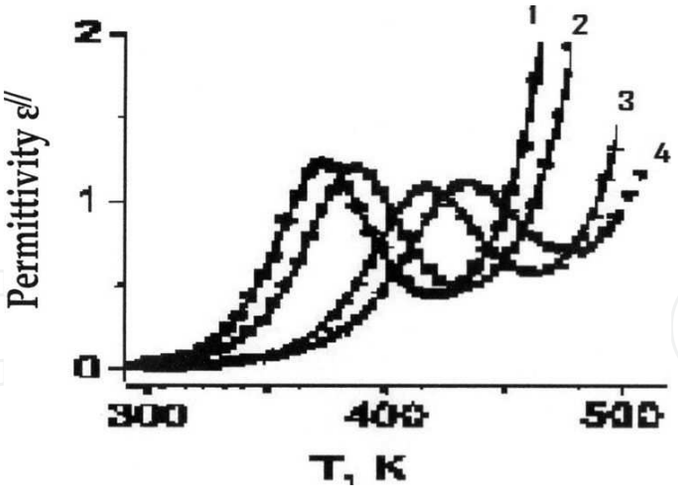

Figure 8. Temperature dependence of Imaginary part $\varepsilon''$of permittivity $\varepsilon=\varepsilon'-j\varepsilon''$ of LGO:Cr^{3+}, measured along crystal a -axis at the following frequencies : 0.5 kHz (1); 1 kHz (2); 5 kHz (3); 10 kHz (4). Distinct peak is observed in ε'' in the temperature range 350-450 K and the peak is observed to shift to higher temperature for higher frequencies. In contrast no such peak is observed for the real part ε' of the permittivity. The typical behavior is observed only along crystal a –axis which incidentally coincides with the proposed Cr^{3+}- Li^{+} centers.

1.4. Principle of Photoelasticity

If a rectangular parallelepiped with edges parallel to x[100], y[010] and z[001] axes is stressed along z-axis and observation is made along y-axis, as shown in Fig.9, then the path retardation δ_{zy} introduced per unit length due the stress introduced birefringence is given by

$$\delta_{zy} = (\Delta n_z - \Delta n_x) = C_{zy} P_{zz} \tag{1}$$

where Δn_z and Δn_x are the changes in the corresponding refractive indices, $(\Delta n_z - \Delta n_x)$ is the corresponding stress induced birefringence, P_{zz} is the stress along z-axis and C_{zy} is a constant called the Brewster constant or the relative photoelastic coefficient. In general the Brewster constant is related to the stress optical and strain optical tensors of forth rank [39] and is a measure of the stress induced (piezo-optic) birefringence. It is conveniently expressed in the unit of 10^{-13} cm^2/dyne per cm thickness along the direction of observation is called a Brewster [39].

1.5. Measurement procedure of photoelastic constants

To study the piezo-optical birefringence the experimental set up consists of a source of light (S), a lens (L) to render the rays parallel, a polarizer (P), an analyzer Polaroid (A), a Babinet compensator (B) and a detector (D), as shown in Fig.10. The P and A combination are adjusted for optimal rejection of light. The sample with stressing arrangement and a Babinet compensator are placed between P and A. A monochromator and a gas flow temperature controlling device are used to obtain the piezo-optic coefficients (C_λ) at different wavelengths and temperature. The subscript λ in the symbol C_λ denotes that the piezo-optic coef-

ficient depends on the wavelength of light used to measure it. The experiments are carried out for different wavelengths using white light and a monochromator and the monochromatic sodium yellow light. An appropriate stress along a desired direction of the sample is applied with the help of a stressing apparatus comprising a mechanical lever and load.

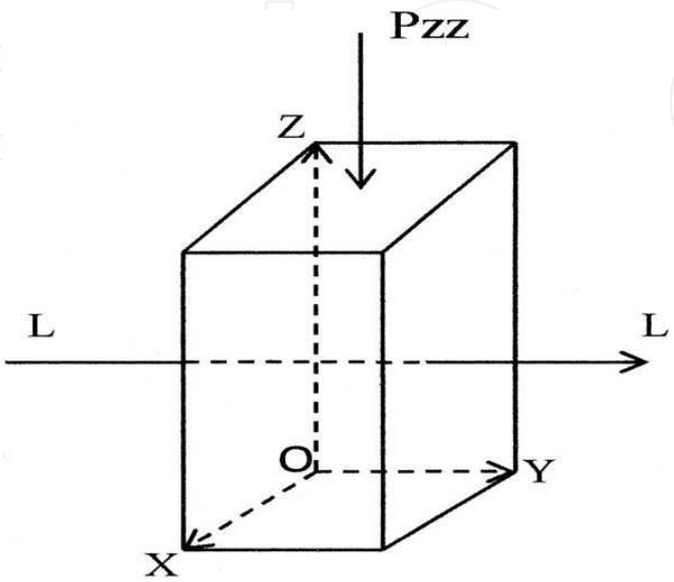

Figure 9. A solid under a linear stress of stress-optical measurements (P_{zz} is the applied stress and LL is the direction of light propagation and observation).

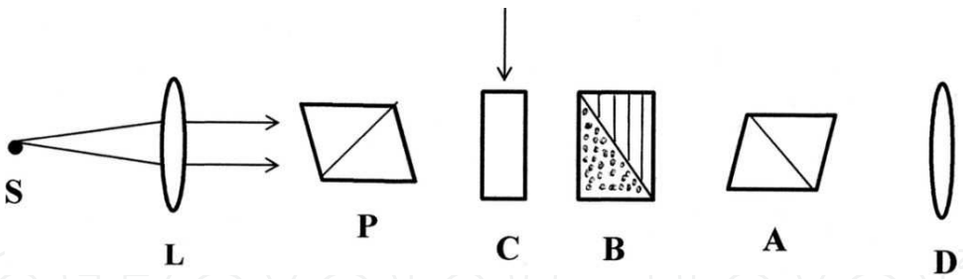

Figure 10. A schematic diagram of the experimental setup for the measurement of photoelastic constants of the crystals at room temperature. Source of light (S), Lense (L), Polarizer (P), Crystals (C) under stress, Babinet Compensator (B), Analyzer (A) and Detector (D).

To start with, the Babinet compensator is calibrated and the fringe width is determined for different wavelengths of light in the visible region. The crystal specimen is placed on the stressing system so that the stress could be applied along vertical axis and observation made along horizontal axis. A load on the crystal shifts the fringe in the Babinet compensator and this shift is a measure of the piezo-optic behavior. The piezo-optic coefficients (C_λ) are now calculated using the calibration of the Babinet compensator. The experiment is repeated for other orientations of the crystals and the results are obtained.

http://dx.doi.org/10.5772/52098

1.6. Piezo-optic Dispersion of $Li_2Ge_7O_{15}$ Crystals

The experimental procedure for the piezo-optic measurements is described in section 1.5. The polished optical quality samples worked out to dimensions i) 5.9 mm, 9.4 mm and 5.0 mm; ii) 3.17 mm, 5.88 mm and 6.7 mm, along the crystallographic a, b and c axes respectively. The stress was applied with an effective load of ~23 kg in each case [40].

The values of C_λ thus obtained at different wavelengths are given in Table 2 and the results are plotted in Fig. 11. Here C_{pq} is the piezo-optic coefficient with the stress direction being p and observation direction being q. The results show an interesting piezo-optic behavior. A survey of literature indicates that the piezo-optic behavior of materials studied till now shows a reduction of C_λ with increasing wavelength in the visible region [39]. In the present case, C_λ decreases with wavelength up to a certain wavelength as in other normal materials and then suddenly shows a peak and later on the usual behavior of reduction in the values of piezo-optic coefficients is observed.

		Wavelengths				
Obs.	C_{pq}	4358**Å**	4880**Å**	5390**Å**	5890**Å**	6140**Å**
1	C_{xy}	4.024	3.819	3.722	4.328	3.677
2	C_{xz}	5.243	4.895	4.770	5.552	4.451
3	C_{yx}	4.084	3.525	3.092	3.562	2.913
4	C_{yz}	4.353	4.118	3.946	4.261	3.866
5	C_{zy}	4.179	2.814	3.177	3.713	3.172
6	C_{zx}	3.312	2.991	2.650	4.190	2.618

Table 2. Stress optical coefficients c_{pq} (in Brewster) for $Li_2Ge_70_{15}$ at different wave lengths.

To the best knowledge of the authors this behavior is unique to the LGO crystals. For the sake of convenience we denote C_λ measured at λ = 5890 Å as C_{5890} and so on. The results show that sometimes the value of C_{5890} is even higher than that at C_{4400}, the value of piezo-optic coefficient obtained at the lowest wavelength studied here. This is the case with C_{xy}, C_{zx} and C_{xz}. For other orientations the value is lower than that at 4400 Å. Further, C_λ is found to have increased to more than 50% in the case of stress along [001] and observation along [100]. Also, it is interesting to note that the value of C_{6140}, is less than that of C_{5390}, in tune with usual observation of piezo-optic dispersion. Thus one can see an "optical window" in between 5400 Å and 6200 Å. The height of this optical window is different for various orientations, though the width seems approximately the same. The maximum height of about 1.5 Brewster was found for C_{zx} followed by C_{xz} with about 0.9 Brewster. It should be noted here that z-axis is the ferroelectric axis for LGO. It is also interesting to note that the change in height is more in the former while the actual value of C_λ, is less compared to that of the latter. The percentage dispersion also is different for various orientations. It is very high, as high as 25% for C_{zy}, while it is just 10% for C_{xy}.

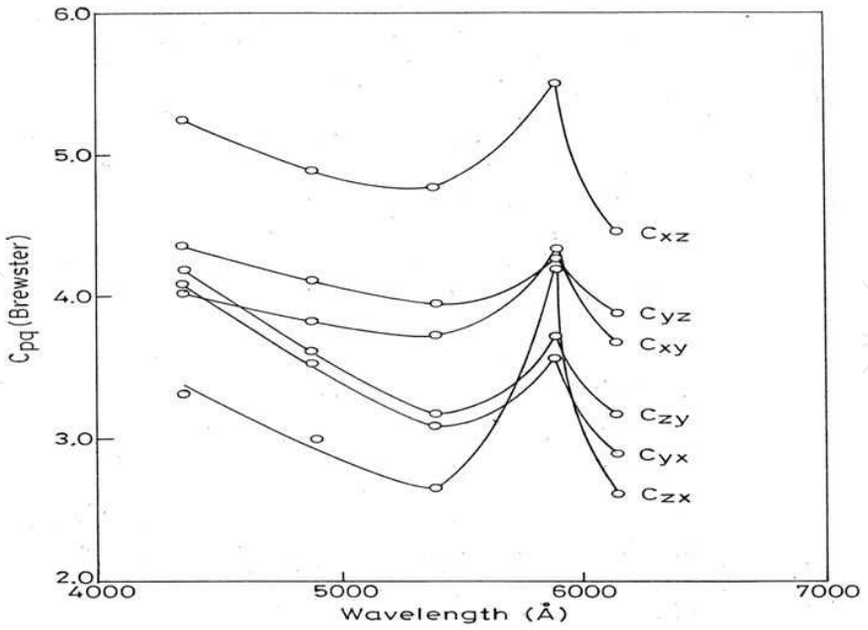

Figure 11. Stress optical dispersion of $Li_2Ge_70_{15}$ crystals with wavelength at room temperature (298 K).

Figure 12 shows the variation of $C_{zx}(\lambda)$ at the temperatures ranging from 298K to 283K on cooling process of the sample LGO. It is clear from the figure that the distinct peak of $C_{zx}(\lambda)$ appears only at the sodium yellow wavelength of 5890 Å for the whole range of temperatures (298 K–283 K) investigated. It is also interesting to note that a temperature anomaly is also observed around 283 K. LGO undergoes a second order phase transition at 283.5 K from the high temperature paraelectric phase to the low temperature ferroelectric phase. So this anomaly is related to this phase transition of the LGO crystal.

The observed peculiarity of piezo-optic behavior could be due to many factors, viz., i) anomalous behavior of refractive index or birefringence ii) anomalous ferroelastic transformation at some stage of loading iii) shift of absorption edge due to loading. The following have been done to identify the reasons for this peculiar behaviour.

Birefringence dispersion has been investigated in the visible region and no anomalies in its behavior has been observed. This rules out the first of the reasons mentioned. The reason due to ferroelastic behavior also is ruled out since the effect would be uniform over all the wavelengths investigated. It was not possible to investigate the effect of load on the absorption edge. Hence an indirect experiment has been performed. If there is a shift in the absorption edge due to loading the sample, the peak observed now at sodium yellow light would shift with load. No clear shift of the peak could be observed within the experimental limits. Another interesting experiment was done to identify the source of the anomaly. It is well known that T_c of LGO changes under uniaxial stress. The measurements were made near T_c under different stress (loads). Although T_c was found to shift a little with load the dispersion peak did not show any discernible shift. No particular reason could be established as to why a dispersion peak appears around sodium yellow region. Another interesting work in this

http://dx.doi.org/10.5772/52098

direction is on $Gd_2(Mo0_4)_3$ — where an anomalous peak was recorded in spontaneous birefringence at 334.7 nm [41], an observation made for the first time.

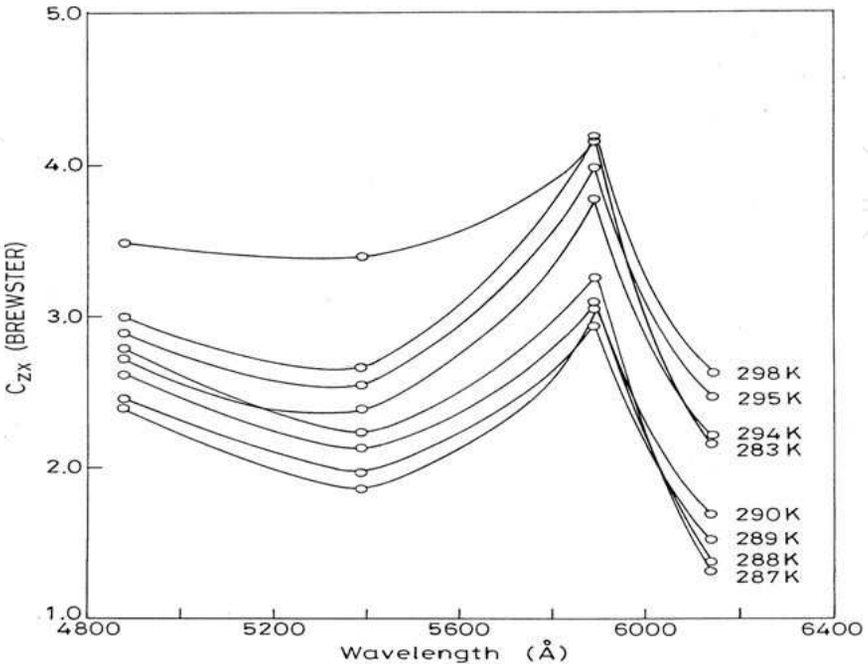

Figure 12. The variation of $C_{zx}(\lambda)$ at the temperatures ranging from 298 K to 283 K on cooling process of the sample $Li_2Ge_70_{15}$.

It is well known that the photoelasticity in crystals arises due to change in number of oscillators, effective electric field due to strain and the polarisability of the ions. In the present case, as the wavelength approaches around 5400 Å, the ionic polarisability seems to be changing enormously. There is no optical dispersion data available on LGO. We have conducted an experiment on transmission spectra of LGO along x, y and z-axes, which shows a strong absorption around 5400 Å. The observed anomaly in the piezo-optic dispersion may be attributed to the absorption edge falling in this region. This explanation needs further investigation in this direction. It is also known that the strain optical dispersion arises due to the shift in absorption frequencies and a change in the oscillator strength caused by the physical strain in the crystal.

1.7. Irradiation Effect on Piezo-optic Dispersion of $Li_2Ge_7O_{15}$ Crystals

The ferroelectric single crystals $Li_2Ge_7O_{15}$ was irradiated by x-ray for one hour and the experimental processes described in section 1.5 were repeated for the crystal (irradiated) LGO in order to understand the radiation effect on piezo-optical birefringence dispersion [18]. The values of C_λ of the crystal (irradiated) LGO thus obtained at different wavelengths are given in Table 3 and the results are plotted in Fig. 13.

		Wavelengths				
Obs.	C'_{pq}	4358**Å**	4880**Å**	5390**Å**	5890**Å**	6140**Å**
1	C'_{xy}	4.08	3.87	3.72	4.33	3.73
2	C'_{xz}	5.35	5.00	4.88	5.59	4.55
3	C'_{yx}	4.02	3.47	3.01	3.50	2.83
4	C'_{yz}	4.39	4.19	4.01	4.26	3.90
5	C'_{zx}	4.63	4.46	4.41	4.66	4.29
6	C'_{zy}	3.71	3.26	2.97	3.43	2.72

Table 3. Stress Optical Coefficients C_{pq} (in Brewsters) for $Li_2Ge_70_{15}$ (irradiated) at different wavelengths.

Some interesting results are obtained in the case of irradiated crystal LGO. The peak value of C'_{zx} has decreased about 18% and that of C'_{zy} has increased about 25% at the wave length λ= 5890 Å. Also, it is interesting to note that the value of C_{6140}, is less than that of C_{5390} for the un-irradiated and irradiated sample of LGO crystal, in tune with usual observation of piezo-optic dispersion.

Irradiation of crystals can change physical properties of the crystals. Irradiation brings about many effects in the crystal such as creating defects, internal stress and electric fields etc. These irradiation effects in turn are supposed to affect the physical properties of the irradiated crystal as compared to un-irradiated crystal. While there was no appreciable change in the lattice parameters, a significant drop in the value of dielectric constant and tan δ was observed upon x-irradiation of ferroelectric glycine phosphate. An appreciable shift in the phase transition temperature towards the lower temperature was observed. These changes are attributed to the defects produced in it by irradiation [42]. The studies of triglycine sulphate (TGS) showed that very small doses of x-irradiation can give large changes of the ferroelectric properties. The direct evidence of domain clamping by defects was obtained from optical studies. With increasing dosage the dielectric constant peak and polarization curve broaden and move to lower temperatures. In our present studies, the x-irradiation is believed to produce internal stress and electric fields inside the crystals LGO due to defects that can change the values of piezo-optic constants [43].

1.8. Piezo-optic Birefringence in $Li_2Ge_7O_{15}$ Crystals

The temperature dependence of the photoelastic coefficients of the ferroelectric crystals $Li_2Ge_7O_{15}$ in a cooling and heating cycle between 298 K and 273 K was carried out with the experimental procedure described in section 1.5 [19]. A special arrangement was made to vary the temperature of the sample. The temperature was recorded with a digital temperature indicator and a thermocouple sensor in contact with the sample.

http://dx.doi.org/10.5772/52098

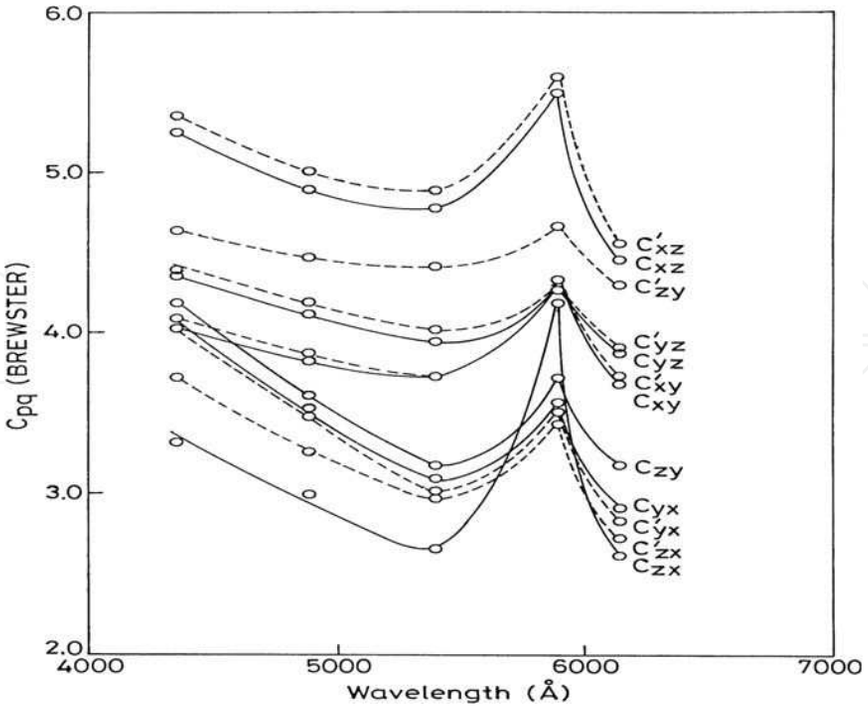

Figure 13. Stress optical dispersion of $Li_2Ge_70_{15}$ crystals (un-irradiated and irradiated) with wavelength at room temperature (298 K).

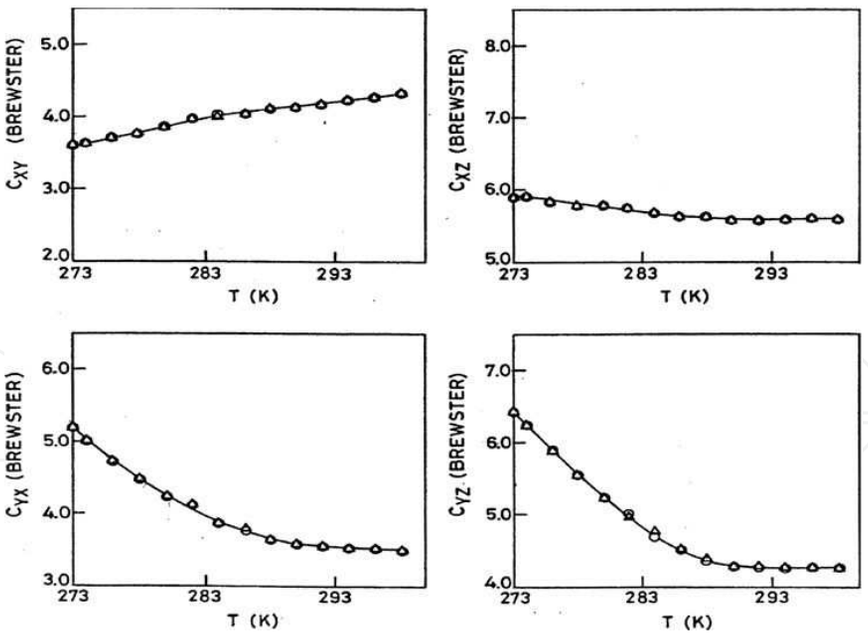

Figure 14. Temperature dependence of the piezo-optic coefficients C_{xy}, C_{xz}, C_{yz} and C_{yx} of the crystals LGO in a cooling (0) and heating (Δ) cycle.

The temperature dependence of piezo-optic coefficients C_{pq} of the crystals $Li_2Ge_7O_{15}$ between 298 K and 273 K were determined and are shown in Fig. 14 and Fig. 15. The values of C_{pq} at

291 K and 278 K were reported in paper [44] and it was observed that there were large changes in the values of C_{zy} and C_{yz} at 278 K and 291 K as compared to other components and C_{zy} did not show a peak in its temperature dependence between 291K and 278 K.

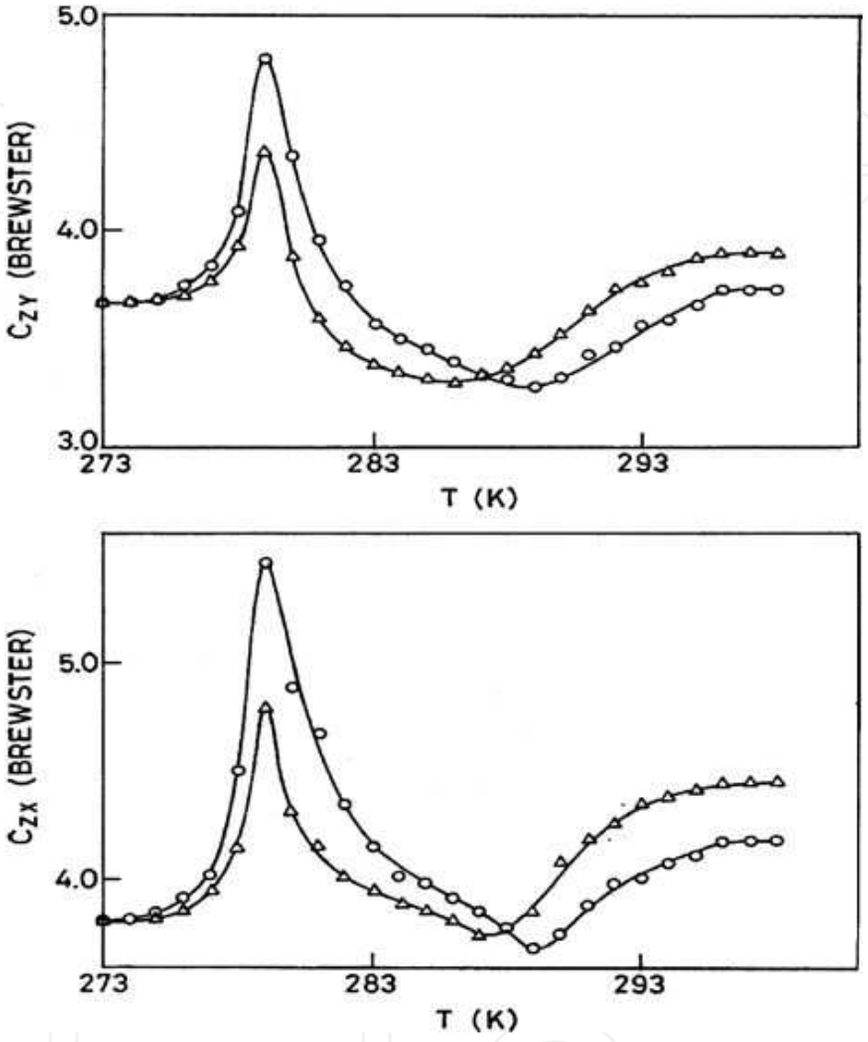

Figure 15. Anomalous temperature dependence of the piezo-optic coefficients C_{zx} and C_{zy} of the crystals LGO in a cooling (0) and heating (Δ) cycle.

Here in contrast we observed a peak in the temperature dependence of both C_{zy} and C_{zx} at 279 K. The temperature dependence of C_{pq} are quite interesting, for example the piezo-optic coefficients C_{yz}, C_{yx} and C_{xz} have negative temperature derivatives but C_{xy} has a positive temperature derivative. In complete contrast both C_{zy} and C_{zx} have both positive and negative temperature derivatives at different temperature intervals between 298 K and 273 K (Table: 4). Besides a clear thermal hysteresis is observed in C_{zy} and C_{zx} in a complete cooling and heating cycle (Fig. 15) whereas no discernible hysteresis is observed in rest of the piezo-optic coefficients (Fig. 14). The two distinct anomalies in the temperature dependence of C_{zy} and C_{zx} are characterized by a valley at T_m (~289 K) and a peak at T_c (~279 K). Anomalous temperature dependence of C_{zx} at different wave lengths is also shown in Fig. 16. The tem-

http://dx.doi.org/10.5772/52098

perature dependence of the dielectric permittivity along the c-axis of LGO shows a sharp peak at T_c (283.5 K) and the Curie-Weiss law holds only for a narrow range of temperature ($T_c \pm 4$ K) [11,15, 16]. The peak for piezo-optic coefficient is attributed to the paraelectric to ferroelectric phase transition of LGO at T_c. To check the curie-Weiss law like dependence near T_c the following relation is used.

$$C^T_{pq} - C^0_{pq} = K_{pq} / (T - T_c) \quad (2)$$

Where C^T_{pq} and C^0_{pq} denote the value of the corresponding piezo-optic coefficients at temperature T and 273 K respectively and K_{pq} is a constant. Fig. 17 shows the $(C^T_{pq} - C^0_{pq})^{-1}$ vs $(T-T_c)$ curve for C_{zx} and C_{zy}. It is clear from these curves that like dielectric constant the relation fits well only within a narrow range of temperature near $T_c(T_c \pm 4$ K). The solid lines denote the theoretical curves with the following values $K_{zx} = 1.05$; $K_{zy} = 0.92$ for $T > T_c$, $K_{zx} = -0.40$; $K_{zy} = -0.34$ for $T < T_c$ and $T_c = 279$ K.

C_{pq}	Value of Derivative (Brewster/K)	Temperature Range Ratio
C_{zx}	0.013	296K-289K -1.69
	-0.022	289K-283K
	-0.090	282K-279K -2.0
	0.181	279K-276K
	~0	276K-273K
C_{xz}	-0.003	293K-273K
C_{zy}	0.020	296K-289K -0.75
	-0.015	289K-283K
	-0.095	282K-279K -1.9
	0.179	279K-276K
	~0	276K-273K
C_{yz}	-0.026	293K-273K
C_{xy}	0.007	293K-273K
C_{yz}	-0.023	293K-273K

Table 4. The temperature derivative $[dl_nC_{pq}/dT]$ of the piezo-optic coefficients of $Li_2Ge_7O_{15}$.

Furthermore the magnitudes of the ratio of the temperature derivatives below and above T_m and T_c are given in Table 4 and we can see that the ratio near T_c comes out to be about 2. Therefore it satisfies the law of two for the ratio of such derivatives of quantities which are coupled with the spontaneous polarization in second order ferroelectric phase transition such as in the case of triglycine sulphate [45] and LGO. Therefore the peak around T_c is [13, 15, 16] attributed to the paraelectric to ferroelectric phase transition of LGO. The smallness

of K_{pq} and the applicability of relation (2) above only in a narrow range of temperature suggest that LGO may be an improper ferroelectric. The law of two does not hold for the ratio at T_m (Table 4). Therefore this anomaly is not related to the spontaneous polarization.

From the behaviour that only C_{zx} and C_{zy} show anomalous it is obvious that birefringence $(\Delta n_z - \Delta n_y)$ and $(\Delta n_z - \Delta n_x)$ show steep increase around T_c and below T_c show a $(T-T_c)^{1/2}$ behaviour correlated to the spontaneous polarization which is parallel to the z-axis (crystallographic c-axis). From the behaviour of C_{xy} and C_{yx} which do not show any temperature anomaly we may say that only n_z is responsible for the anomaly in accordance with the behaviour of the dielectric properties where only ε_{33} is strongly affected by the phase transition. These observations are in accordance with the results of Faraday effect and birefringence in LGO [13].

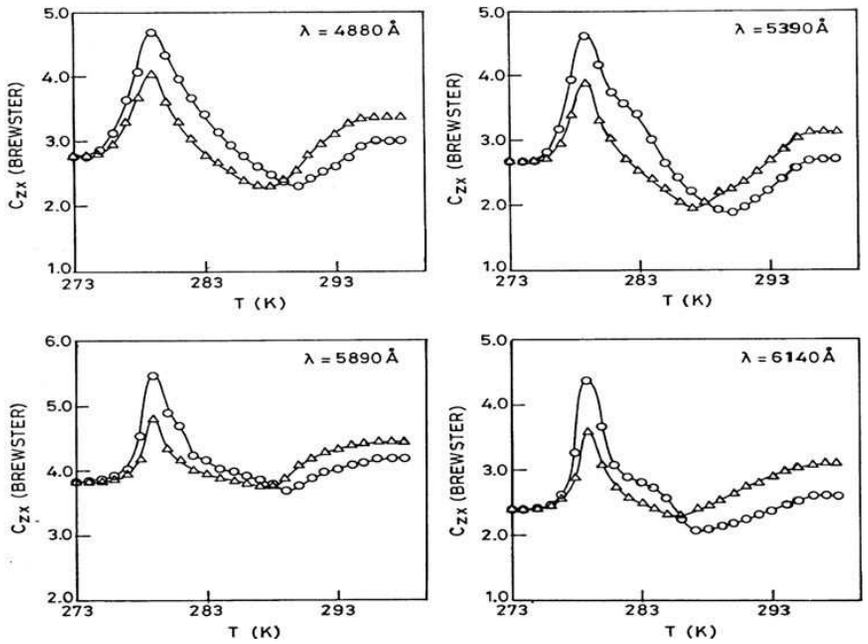

Figure 16. Anomalous temperature dependence of piezo-optic coefficient C_{zx} of the crystals LGO at different wave lengths in a cooling (0) and heating (Δ) cycle.

As mentioned by Lines and Glass [43], under an external pressure T_c of a ferroelectric phase transition may be shifted. This shift may be to the higher or the lower side of normal T_c. Wada et al. [46] studied the pressure effect on the ferroelectric phase transition in LGO through the dielectric and Raman scattering measurements and found a positive pressure coefficient dT_c/dp = 14.6 K/kbar. Preu and HaussÜhl [12] studied the dependences of dielectric constants on hydrostatic and uniaxial pressure as well as temperature. They observed a shift of T_c at a rate of 14.02 K/kbar for the hydrostatic pressure and ~7 K/kbar for the uniaxial pressure. In the present case the position of the peak of C_{zy} is found to depend on the stress applied. If the peak position is believed to represent the T_c, it appears to shift to the lower side under the uniaxial stress. To see whether T_c shifts linearly with uniaxial stress similar to the earlier observations [12, 46], we used different stresses within the elastic limits of LGO for

http://dx.doi.org/10.5772/52098

C_{zx} and found a linear relationship (Fig. 18). However, a negative stress coefficient $dT_c/dp \sim -22$ K/kbar is obtained in this case which agrees only in magnitude with the hydrostatic pressure coefficient. The linear curve (Fig. 18) extrapolates to a $T_c = 281.5$ K in the unstressed state instead of 283.5K as determined by dielectric measurements [11, 15, 16]. This may be due to a non linear dependence of shift of T_c under stress near 283.5 K.

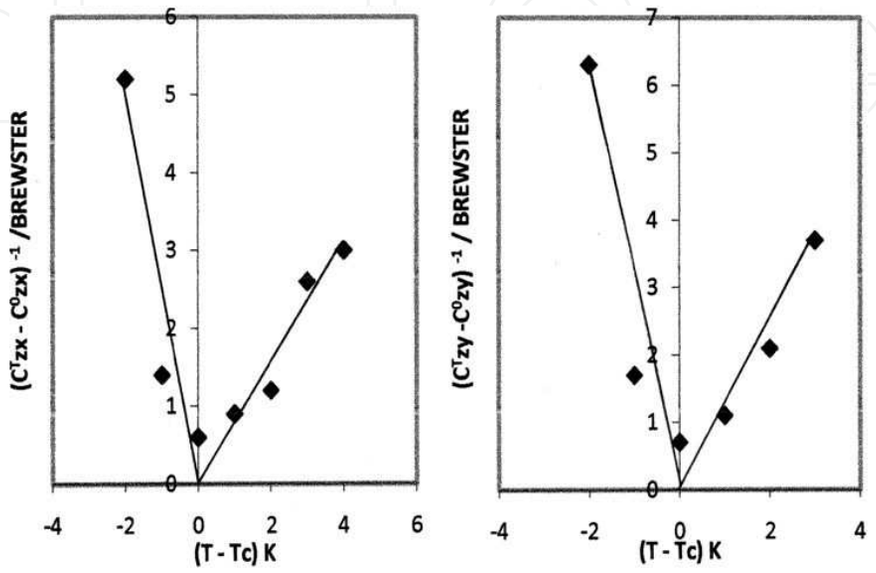

Figure 17. Plots of $(C^T_{pq} - C^o_{pq})^{-1}$ vs $(T-T_c)$ curve for C_{zx} and C_{zy}.

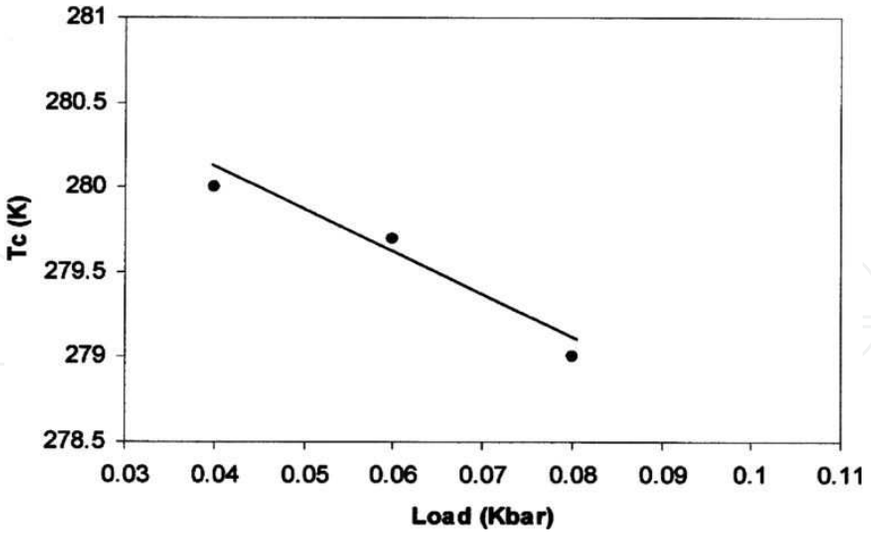

Figure 18. The stress dependence of the shift of T_c for C_{zx}.

Now we turn to the anomaly around T_m. Morioka et al. [47] proposed that there is an interaction between the soft phonon mode and a relaxational mode in the paraelectric phase in the temperature interval 300 K to T_c. The critical slowing down of the relaxational mode

near T_c is expected to cause the increase of the fluctuation of the spatially homogeneous polarization and thereby the increase of the fluctuation of the hyperpolarizability with $k_c = 0$. Wada et al. [48] measured the soft phonon mode with the help of their newly designed FR-IR spectrometer and proposed that as T_c is approached from above soft phonon mode becomes over damped and transforms to a relaxational mode.

On the other hand there may exist a relaxational mode with an independent degree of freedom as well as the soft phonon mode and the character of the softening transfers from the phonon to the relaxational mode. This is an important problem in determining the dynamics of the peculiar ferroelectric phase transition of LGO, where both the dielectric critical slowing down characteristic of the order-disorder phase transition and the soft phonon mode characteristic of the displacive phase transition are observed [11, 14]. In the light of the above discussion we may say that the change up to T_m is caused by the softening of mode and the softening character transforms to the relaxations mode near T_m causing a change in the trend below T_m and near T_c the relaxational mode becomes dominant. The valley around T_m is perhaps caused by the interplay between the competitive relaxational mode and the soft phonon mode. It has been observed that softening of the velocity and rise of the damping of acoustic phonon occur in the paraelectric phase of LGO even quite far from T_c, i.e.$(T-T_c) \sim 30$ K and the effect is attributed to the fluctuation induced contributions [49].

Obs.	Cpq	Paraelectric (PE) phase (RT)	At T_c = 279 K
1	C_{xy}	4.38	3.85
2	C_{xz}	5.55	5.85
3	C_{yx}	3.60	4.46
4	C_{yz}	4.26	5.50
5	C_{zy}	3.71	4.83
6	C_{zx}	4.19	5.45

Table 5. Stress optical coefficients c_{pq} (in Brewster's) of $Li_2Ge_7O_{15}$ at RT=298 K and at T_c = 279 K.

Another interesting aspect is the observation of a significant thermal photoelastic hysteresis (Fig. 15). Although the peak position does not shift in the heating cycle the values of the photoelastic constants get reduced significantly in the heating cycle as compared to the corresponding values in a cooling cycle. A similar kind of hysteresis was observed in the dielectric behaviour of LGO and the appearance of the dielectric hysteresis is attributed to the internal space charge (electrets state) effects which produce an internal electric field in LGO on heating from the ferroelectric phase [15-17]. It was possible to compensate the internal electric field effects in dielectric measurements by an external electric field [15-17]. It is suspected that the photoelastic hysteresis also occurs due to similar effects. Although it was not possible to try to compensate the electric field effects in the present investigation, it is possi-

http://dx.doi.org/10.5772/52098

ble to attempt experiment under the simultaneous application of a suitable electric field and stress along z-direction.

Obs	C_{pq}	Rochelle (RS)	SaltKDP	ADP	Remarks
1	C_{xz}	3.74	0.28	1.25	Ref. [50] for RS
2	C_{yz}	4.29	0.28	1.25	a- polar axis
3	C_{yx}	3.56	1.04	4.30	Ref. [51] for KDP
4	C_{zx}	0.85	1.54	3.50	Ref. [52] for ADP
5	C_{zy}	2.61	1.54	3.50	
6	C_{xy}	3.04	1.04	4.30	

Table 6. Piezo-optic coefficients c_{pq} (in Brewsters) for some ferroelectric crystals in their paraelectric (PE) phases.

The Stress optical coefficients C_{pq} of the crystals $Li_2Ge_7O_{15}$ at paraelectric phase (RT = 298 K) and at T_c = 279 K are presented in Table 5. It is important to compare the values of C_{pq} for $Li_2Ge_7O_{15}$ with other ferroelectric crystals given in Table 6 particularly with Rochelle-salt (RS) which belongs to the orthorhombic class like LGO [44]. The values of C_{pq} are significantly higher for LGO as compared to these ferroelectric systems. So, the large photoelastic coefficients and the other properties like good mechanical strength, a transition temperature close to room temperature and stability in ambient environment favour LGO as a potential candidate for photoelastic applications.

The EPR (Electron Paramagnetic Resonance) spectroscopy of the transition metal ion doped crystals of LGO (Mn^{2+}, Cr^{3+}) has also been studied both in Paraelectric (PE) and ferroelectric (FE) phases in the temperature interval from 298 K to 279 K during cooling and heating cycles [17, 36, 53]. It is observed that on approaching T_c in a cooling cycle, the EPR lines are slightly shifted to the high field direction and undergo substantial broadening. At the temperature T_c (≈ 283.4 K), the EPR lines are splitted into two components which are shifted to the higher and lower field directions progressively as a result of cooling the sample below T_c as shown in Fig.19.

During heating cycle (i.e. approaching T_c from below), the phenomena occurred were just opposite to the above processes observed in the cooling cycle. However, the EPR line width (peak to peak ΔH_{pp}) for H ∥ c, $H_{\perp}$a was found to decrease to about one third of its value at T_c in a heating cycle as compared to its value in the cooling cycle. The shape of the EPR resonance lines far from T_c has a dominant Lorentzian character (a Lorentzian line shape) but very near to T_c, the line shape has been described mainly by Gaussian form of distribution (a Gaussian line shape). All the peculiarities observed are attributed to the PE ↔ FE phase transition of the LGO crystals. The line width reduction near T_c is attributed to the internal space charge (electret state) effects which produce an internal electric field inside the crystals

on heating process from the ferroelectric phase. This observation is similar to the photoelastic hysteresis behavior of the crystals LGO near T_c.

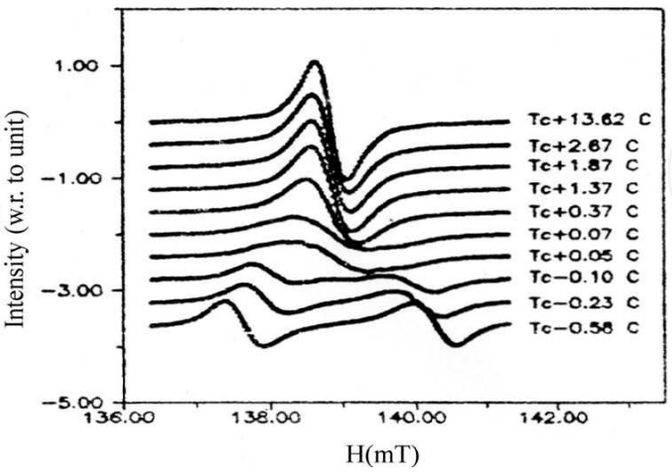

Figure 19. Temperature dependence of EPR lines of $Li_2Ge_7O_{15}:Cr^{+3}$ crystals for |M|= ½ ⟷3/2, H ∥ a, $H_{\perp}c$ near T_c during cooling process.

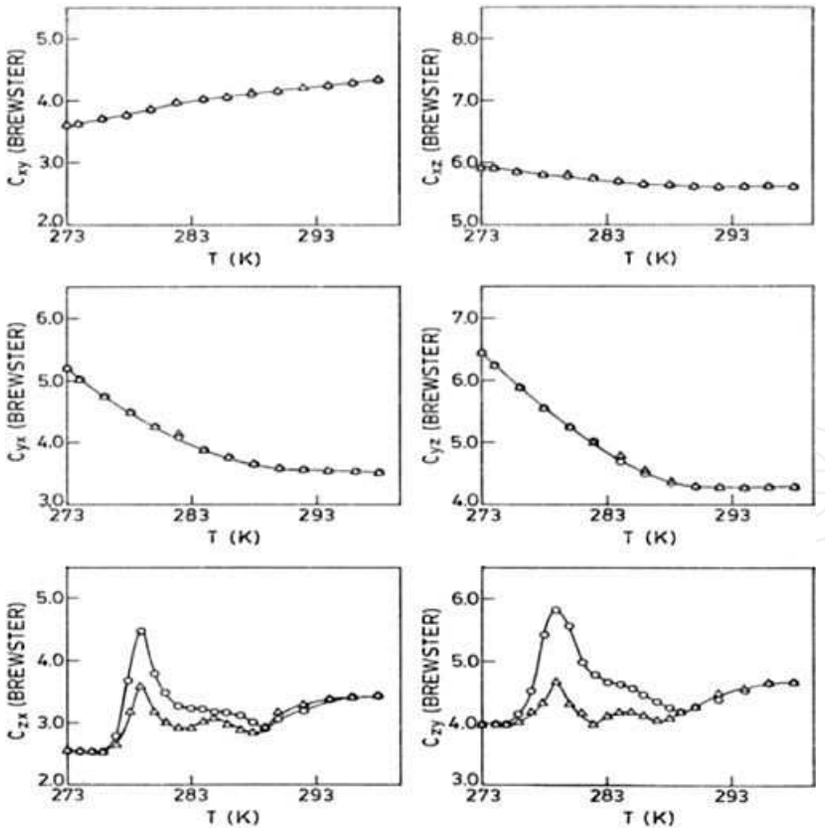

Figure 20. Temperature dependence of photoelastic coefficients C_{xy}, C_{xz}, C_{yz}, C_{yx}, C_{zx} and C_{zy} of the crystal (x-irradiated) LGO in a cooling (0) and heating (Δ) cycle.

http://dx.doi.org/10.5772/52098

1.9. Irradiation Effect on piezo-optic Birefringence in $Li_2Ge_7O_{15}$ Crystals

The photoelastic coefficients C_{pq} of the ferroelectric crystals $Li_2Ge_7O_{15}$ (x-irradiated) in a cooling and heating cycle between 298 K and 273 K was carried out with the experimental procedure described in section 1.5 and are shown in Fig. 20 [54]. The results show an interesting photoelastic behaviour.

Peaks are observed in the temperature dependence of the photoelastic coefficients C_{zy} and C_{zx} at temperature ~ 279 K in a complete cooling and heating cycle whereas no discernible hysteresis is observed in rest of the photoelastic coefficients. Anomalous temperature dependence of C_{zx} of the crystal (x-irradiated) LGO at different wave lengths are shown in Fig.21.

It is observed that the peak value of C_{zy} has increased about 25% and that of C_{zx} has decreased about 18% at the wave length λ=5890 Å during cooling process of the crystal (Fig.15 and Fig.20). The peak value of C_{zx} of the crystal (un-irradiated and x-irradiated) LGO thus obtained at different wave lengths (Fig.16 and Fig.21) are given in Table 7 and the results are plotted in Fig.22.

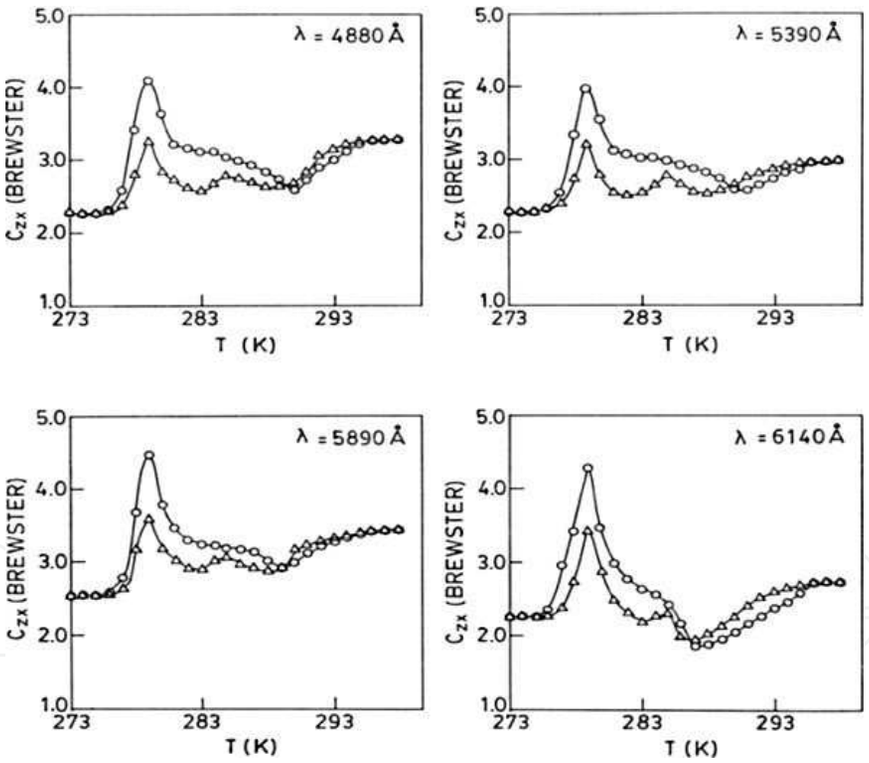

Figure 21. Temperature dependence of photoelastic coefficient C_{zx} of the crystal (x-irradiated) LGO at different wave lengths in a cooling (0) and heating (Δ) cycle.

It has been observed that the changes in the value of photoelastic coefficients C_{zy} and C_{zx} of the crystal (x-irradiated) LGO in a cooling and heating cycle occur only if the crystal is stressed along the polar axis (z-axis). It is known that the irradiation of crystals can change physical properties of the crystals.

Wave lengths	C_{zx} (un-irradiated)		C_{zx} (x-irradiated)	
(Å)	Cooling	Heating	Cooling	Heating
4880	4.8	4.0	4.05	3.3
5390	4.7	3.9	3.95	3.2
5890	5.6	4.8	4.6	3.7
6140	4.5	3.6	4.3	3.4

Table 7. The peak value of C_{zx} (in Brewster) for the Crystal (un-irradiated and x-irradiated) LGO at different wave lengths in the cooling and heating cycles.

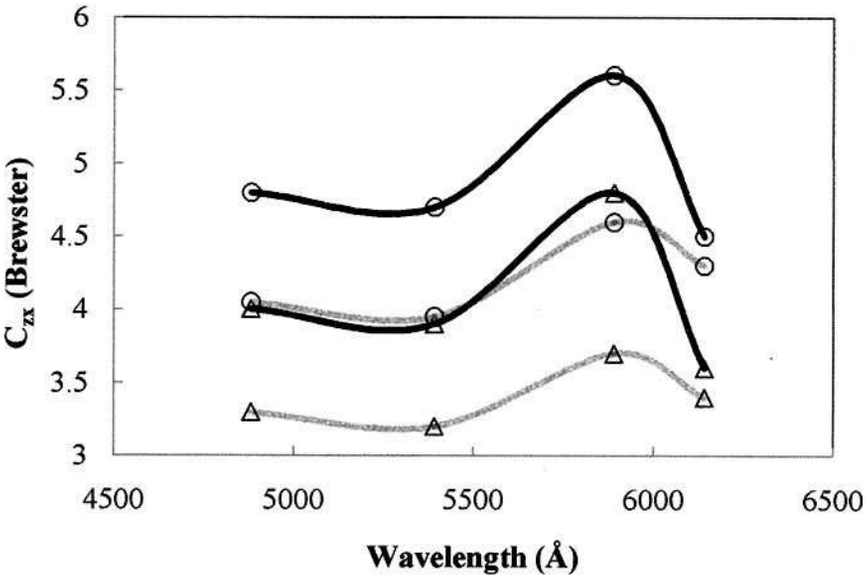

Figure 22. The peak value of C_{zx} for the un-irradiated (black colour) and x-irradiated (ash colour) crystal LGO at different wave lengths in a cooling (0) and heating (Δ) cycle.

Irradiation brings about many effects in the crystal such as creating defects, internal stress and electric fields etc [43]. In our present studies, the x-irradiation is believed to produce internal stress and electric fields inside the crystals $Li_2Ge_7O_{15}$ due to defects that can change the values of photoelastic coefficients.

2. Summary

It is known that the Barium strontium titanate $Ba_{1-x}Sr_xTiO_3$(BST) is one of the most interesting thin film ferroelectric materials due to its high dielectric constant, composition dependent curie temperature and high optical nonlinearity. The wavelength dependence of refractive index of BST ($Ba_{0.05}Sr_{0.95}TiO_3$) thin films has shown a nonlinear dependence in the 1450-1580 nm wavelength range at room temperature as described in section 1.1. The dispersion curve decreases gradually with increasing wavelength. The average value of the refrac-

http://dx.doi.org/10.5772/52098

tive index is found to be 1.985 in the 1450-1580 nm wavelength range which is considered to be important for optoelectronic device applications.

The study of fluorescence spectra of the crystals $Li_2Ge_7O_{15}:Cr^{3+}$ in the temperature interval 77-320 K shows the sharply decrease of intensities of the R_1 and R_2 lines (corresponding to the Cr^{3+} ions of types I and II) during cooling process near the temperature T_c = 283.5 K as described in section 1.3. Such nature of suppression of R_1 and R_2 lines was not observed previously and it may be related with the mechanism of interaction of excitation spectra of light in the crystals $Li_2Ge_7O_{15}:Cr^{3+}$ at the temperature T_c. The doping of chromium in LGO is believed to create Cr^{3+}- Li^{+} defect pairs in the host LGO lattice at Ge^{4+} sites creating dipoles in two conjugate directions. The EPR, optical, dielectric and fluorescence studies conform each other and pose more scope for further studies.

The high optical quality, good mechanical strength and stability in ambient environment and large photoelastic coefficients in comparison with other ferroelectric crystals like Rochelle-salt, KDP and ADP favour the crystals LGO as a potential candidate for photoelastic applications. The piezo-optic dispersion of the crystals (un-irradiated and x-irradiated) LGO in the visible region of the spectrum of light at room temperature (298 K) have been described in sections 1.6 and 1.7. It shows an "optical zone or optical window" in between the wavelengths 5400 Å and 6200 Å with an enhanced piezo-optical behavior. This peculiar optical window can have a technical importance for example this window region can act as an optical switch for acousto-optical devices. From the studies undertaken it may be concluded that LGO is an attractive acousto-optic material which deserves further probe. It may be possible to understand the observed behavior if extensive piezo-optic and refractive index data become available over an extended range of wavelengths.

The temperature dependence of the photoelastic coefficients of the crystals (un-irradiated and x-irradiated) LGO in a cooling and heating cycle between room temperature (298 K) and 273 K have shown an interesting observations: lowering of the T_c under uniaxial stress contrary to the increase of T_c under hydrostatic pressure and observation of thermal photoelastic hysteresis similar to dielectric hysteresis behavior as described in sections 1.8 and 1.9. In our studies, the x-irradiation is believed to produce internal stress and electric fields inside the crystals LGO due to defects that can change the values of photoelastic coefficients, as described in sections 1.7 and 1.9.

Author details

A.K. Bain* and Prem Chand

Department of Physics Indian Institute of Technology Kanpur, Kanpur-208016, INDIA

References

[1] Lepingard, F. A., Kingston, J. J., & Fork, D. K. (1996). Second harmonic generation in $LiTaO_3$ thin films by modal dispersion and quasi phase matching. *Appl. Phys. Lett.*, 68, 3695-3697.

[2] Hewing, G. H., & Jain, K. (1983). Frequency doubling in a $LiNbO_3$ thin film deposited on sapphire. *J. Appl. Phys.*, 54, 57-61.

[3] Lee, S. H., Kim, D. W., Noh, T. W., Lee, J. H., Lim, M. J., & Lee, S. D. (1996). Nonlinear optical properties of epitaxial $LiNbO_3$ film prepared by pulsed laser deposition. *J. Korean Phys. Soc.*, 29, S628-S631.

[4] Moon, S. E., Back, S. B., Kwun, S. I., Lee, Y. S., Noh, T. W., Song, T. K., & Yoon, J. G. (2000). Orientational Dependence of Electro-optic Properties of $SrBi_2Ta_2O_9$ Ferroelectric Thin Films. Jpn. J. Appl. Phys., 39, 5916-5917.

[5] Reitze, D. H., Haton, E., Ramesh, R., Etemad, S., Leaird, D. E., & Sands, T. (1993). Electrical and Electro-optic Properties of Single Crystalline, Epitaxial Thin Films Grown on Silicon Substrates. *Appl. Phys. Lett.*, 63(5), 596-598.

[6] ORNL's. *Thin film Waveguide and the Information Highway by Carolyn Krause*.

[7] Varadam, V. K., Varadam, V. V., Selmi, F., Ounaise, Z., & Jose, K. A. (1994). Multilayer Tunable Ferroelectrci Materiasl and Thin Films. SPIE-Int. *Soc. Opt. Eng.*, 2189, 433-447.

[8] Mohammed, M. S., Naik, R., Mantese, J. V., Schubring, N. W., Micheli, A. L., & Catalan, A. B. (1996). Microstructure and ferroelectric properties of fine-grained $Ba_xSr_{1-x}TiO_3$ thin films prepared by metalorganic decomposition. *J. Mater. Res.*, 11, 2588-2593.

[9] Bain, A. K., Jackson, T. J., Koutsonas, Y., Cryan, M., Yu, S., Hill, M., Varrazza, R., Rorison, J., & Lancaster, M. J. (2007). Optical Properties of Barium Strontium Titanate (BST) Ferroelectric Thin Films. *Ferroelectric Letters*, 34, 149-154.

[10] Wada, M., Swada, A., & Ishibashi, Y. (1981). Ferroelectricity and Soft Mode in $Li_2Ge_7O_{15}$. *J. Phys. Soc. Jpn.*, 50(6), 1811-1812.

[11] Wada, M., & Ishibashi, Y. (1983). Ferroelectric Phase Transition in $Li_2Ge_7O_{15}$. *J.Phys. Soc. Jpn .*, 52(1), 193-199.

[12] Preu, P., & Hauss Ühl , S. (1982). Dielectric Properties and Phase Transition in $Li_2Ge_7O_{15}$. *Solid State Commun*, 41(8), 627-630.

[13] Kaminsky, W., & Hauss, Ühl. S. (1990). Faraday effect aid birefringence in orthorhombic $Li_2Ge_7O_{15}$ near the ferroelectric phase transition. *Ferroelectrics Lett.*, 11(3), 63-67.

[14] Hauss, Ühl. S., Wallrafen, F., Recker, K., & Eckstein, J. (1980). Growth, Elastic Properties and Phase Transition of Orthorombic $Li_2Ge_7O_{15}$. *Z.krist.*, 153, 329-337.

[15] Kudzin, A., Yu, Volnyanskii M. D., & Bain, A. K. (1994). Temperature Hysteresis of the Permittivity of $Li_2Ge_7O_{15}$. *Phys. Solid State*, 36(2), 228-230.

[16] Kudzin, A., Yu, Volnyanskii M. D., & Bain, A. K. (1995). Influence of Space Charges on Ferroelectric Property of Weak Ferroelectric $Li_2Ge_7O_{15}$. *Ferroelectrics*, 164(1), 319-322.

[17] Bain, A.K. (1994). Study of Pecularities of Ferroelectric Phase Transition of the Crystals $Li_2Ge_7O_{15}$ (Ph.D. Thesis). *Dniepropetrovsk State University, Ukraine*, 128.

[18] Bain, A. K., Chand, P., Rao, K. V., Yamaguchi, T., & Wada, M. (2008). Irradiation Effect on Piezo-optic Dispersion of $Li_2Ge_7O_{15}$ Crystals. *Ferroelectrics*, 377(1), 86-91.

[19] Bain, A. K., Chand, P., Rao, K. V., Yamaguchi, T., & Wada, M. (2009). Anomalous Temperature Dependence of Piezo-optic Birefrigence in $Li_2Ge_7O_{15}$ Crystals. *Ferroelectrics*, 386(1), 152-160.

[20] O'Mahony, M.J. (1988). Semiconductor laser optical amplifers for use in future fiber systems. *J. Light wave Technology*, 6(4), 531-544.

[21] Miranda, F. A., Vankeuls, F. W., Romanofsky, R. R., Mueller, C. H., Alterovitz, S., & Subramanyam, G. (2002). Ferroelectric thin-film based technology for frequency and phase agile microwave communication applications. *Integrated Ferroelectrics*, 42, 131-149.

[22] Tian, H. Y., Luo, W. G., Pu, X. H., Qiu, P. S., He, X. Y., & Ding, A. L. (2001). Synthesis and characteristics of strontium-barium titanate graded thin films at low temperature using a sol-gel technique. *Solid State Communications*, 117, 315-319.

[23] Pontes, F. M., Leite, E. R., Pontes, D. S. L., Longo, E., Santos, E. M. S., Mergulhao, S., Pizani, P. S., Lanciotti Jr, F., Boschi, T. M., & Varela, J. A. (2002). Ferroelectric and optical properties of $Ba_{0.8}Sr_{0.2}TiO_3$ thin film. *J. Appl. Phys.*, 91(9), 5972-5978.

[24] Deineka, A., Jastrabik, L., Suchaneck, G., & Gerlach, G. (2002). Optical Properties of Self-Polarized PZT Ferroelectric Films. *Ferroelectrics*, 273, 155-160.

[25] Gu, Y. Z., Gu, D. H., & Gan, F. X. (2001). Optical Nonlinearity in $PbTiO_3$ Thin Film Deposited on $Al2O_3$ with RF-Sputtering System. *Nonlinear Optics*, 28(4), 283-289.

[26] Fernandez, F. E., Gonzalez, Y., Liu, H., Martinez, A., Rodriguez, V., & Jia, W. (2002). Structure, morphology, and properties of strontium barium niobate thin films grown by pulsed laser deposition. *Integrated Ferroelectrics*, 42, 219-233.

[27] Wohlecke, M., Marrello, V., & Onton, A. (1977). Refractive index of $BaTiO_3$ and $SrTiO_3$ films. *J. Appl. Phys.*, 48, 1748-1750.

[28] Wada, M., Swada, A., & Ishibashi, Y. (1984). The Oscillator Strength of the Soft Mode in $Li_2Ge_7O_{15}$. *J. Phys. Soc. Jpn.*, 53(10), 3319-3320.

[29] Iwata, Y., Shibuya, I., Wada, M., Sawada, A., & Ishibashi, Y. (1987). Neutron Diffraction study of structural Phase Transition in Ferroelectric $Li_2Ge_7O_{15}$. *J. Phys. Soc. Jpn.*, 56(7), 2420-2427.

[30] Wada, M. (1988). Soft Mode Spectroscopy Study of Ferroelectric Phase Transition in $Li_2Ge_7O_{15}$. *Ind. J. Pure and Appl. Phys.*, 26, 68-71.

[31] Galeev, A. A., Hasanova, N. M., Bykov, A. B., Vinokurov, B. M., Nizamutdinov, N. M., & Bulka, G. R. (1990). EPR of Cr^{3+} and Fe^{3+} in $Li_2Ge_7O_{15}$ single crystal. In: Spectroscopy, a crystal chemistry and a realstructure of minerals and their analogues. *Kazan' state university*, 77-87, in Russian).

[32] Basun, S. A., Kaplyanski, A. A., & Feofilov, S. P. (1994). Dipolar centres in $Li_2Ge_7O_{15}$ crystal activated with ($3d^3$) ions: a microstructure and spectroscopic effects of an internal and external electric field. *Solid State Phys.*, 36(11), 3429-3449.

[33] Kaplyanski, A. A., Basun, S. A., & Feofilov, S. P. (1995). Ferroelectric transition induced dipole moments in probe ions in $Li_2Ge_7O_{15}$ crystals doped with Mn^{4+} and Cr^{3+} . *Ferroelectrics*, 169, 245-248.

[34] Iwata, Y., Koizumi, H., Koyano, N., Shibuya, I., & Niizeki, N. (1973). Crystal structure determination of ferroelectric phase of $5PbO_3GeO_2$. *J. Phys. Soc. Jap.*, 35(1), 314-315.

[35] Volnianskii, M. D., Trubitsyn, M. P., & Obaidat, Yahia A. H. (2007). EPR and dielectric spectroscopy of reorienting Cr^{3+}- Li^+ pair centres in $Li_2Ge_7O_{15}$ Crystal. *Condensed Matter Physics*, 10(49), 75-78.

[36] Trubitsyn, M. P., Volnianskii, M. D., & Busoul, I. A. (1998). EPR study of the ferroelectric phase transition in $Li_2Ge_7O_{15}$:Cr^{3+} crystal. *Solid State Phys.*, 40, 6, 1102-1105.

[37] Powell, R.C. (1968). Temperature Dependence of the Widths and Positions of the R Lines in $Li_2Ge_7O_{15}$:Cr^{3+} . *J. Appl. Phys.*, 39, 4517-4521.

[38] Powell, R.C. (1968). Energy Transfer between Chromium Ions in Nonequivalent Sites in $Li_2Ge_7O_{15.}$ *Phys. Rev.*, 173, 358-366.

[39] Narsimhamurty, T.S. (1981). Photoelastic and Electro-optic properties of Crystals. *New York: Plenum Press.*, 514.

[40] Bain, A. K., Chand, P., Rao, K. V., Yamaguchi, T., & Wada, M. (2008). Piezo-optic Dispersion of $Li_2Ge_7O_{15}$ Crystals. *Ferroelectrics*, 366(1), 16-21.

[41] Saito, K., Ashahi, T., Takahashi, N., Hignao, M., Kamiya, I., Sato, Y., Okubo, K., & Kobayashi, J. (1994). Optical activity of $Gd_2(MoO_4)_{3.}$ *Ferroelectrics*, 152(1), 231-236.

[42] Vanishri, S., & Bhat, H. L. (2005). Irradiation Effects on Ferroelectric Glycine Phosphite Single Crystal. *Ferroelectrics*, 323(1), 151-156.

[43] Lines, M. E., & Glass, A. M. (2004). Principles and Applications of Ferroelectrics and Related Materials. *Oxford: Clarendon press*, 680.

[44] Bain, A. K., Chand, P., Rao, K. V., Yamaguchi, T., & Wada, M. (1998). Determination of the Photoelastic Coefficients in Lithium heptagermanate Crystals. *Ferroelectrics*, 209(1), 553-559.

[45] Hauss, Ühl. S., & Albers, J. (1977). Elastic and thermoelastic constants of triglycine sulphate (TGS) in the paraelectric phase. *Ferroelectrics*, 15(1), 73-75.

[46] Wada, M., Orihara, H., Midorikawa, M., Swada, A., & Ishibashi, Y. (1981). Pressure Effect on the Ferroelectric Phase Transition in $Li_2Ge_7O_{15}$. *J. Phys. Soc. Jpn.*, 50(9), 2785-2786.

[47] Morioka, Y., Wada, M., & Swada, A. (1988). Hyper-Raman Study of Ferroelectric Phase Transition of $Li_2Ge_7O_{15}$. *J. Phys. Soc. Jpn.*, 57(9), 3198-3203.

[48] Wada, M., Shirawachi, K., & Nishizawa, S. (1991). A Fourier Transform Infrared Spectrometer with a Composite Interferometer for Soft Mode Studies. *Jpn. J. Appl. Phys.*, 30(5), 1122-1126.

[49] Sinii, I. G., Fedoseev, A. I., & Volnyanskii, M. D. (1990). Relaxation- and fluctuation-induced damping of hypersound in the presence of dispersion. *Sov. Phys. Solid State*, 32(10), 1817-1818.

[50] Narasimamurty, T. S. (1969). Piezooptical constants of Rochelle salt crystals. *Phys. Rev.*, 186, 945-948.

[51] Veerabhadra, Rao K., & Narasimamurty, T. S. (1975). Photoelastic behavior of KDP. *J. Mat. Sci.*, 10(6), 1019-1021.

[52] Narasimamurty, T. S., Veerabhadra, Rao. K., & Petterson, H. E. (1973). Photoelastic constants of ADP. *J. Mat. Sci.*, 8(4), 577-580.

[53] Trubitsyn, M. P., Kudzin, A., Yu, Volnyanski. M. D., & Bain, A. K. (1992). Critical Broadening of EPR lines near the Ferroelectric Phase Transition in $Li_2Ge_7O_{15}:Mn^{2+}$. Sov. Phys. Solid State , 34(6), 929-932.

[54] Bain, A. K., & Chand, P. (2011). Irradiation Effect on Photoelastic Coefficients in Ferroelectric $Li_2Ge_7O_{15}$ Crystals. *Integrated Ferroelectrics*, 124, 10-18.

IntechOpen

IntechOpen